IOP Publishing and International Atomic Energy Agency Nuclear Fusion
Nucl. Fusion **51** (2011) 103014 (13pp) doi:10.1088/0029-5515/51/10/103014

Prospects for pilot plants based on the tokamak, spherical tokamak and stellarator

J.E. Menard[1], L. Bromberg[2], T. Brown[1], T. Burgess[3], D. Dix[4], L. El-Guebaly[5], T. Gerrity[2], R.J. Goldston[1], R.J. Hawryluk[1], R. Kastner[4], C. Kessel[1], S. Malang[6], J. Minervini[2], G.H. Neilson[1], C.L. Neumeyer[1], S. Prager[1], M. Sawan[5], J. Sheffield[7], A. Sternlieb[8], L. Waganer[9], D. Whyte[2] and M. Zarnstorff[1]

[1] Princeton Plasma Physics Laboratory, Princeton, NJ, USA
[2] Massachusetts Institute of Technology, Cambridge, MA, USA
[3] Oak Ridge National Laboratory, Oak Ridge, TN, USA
[4] School of Engineering and Applied Science, Princeton University, Princeton, NJ, USA
[5] Department of Engineering Physics, University of Wisconsin, Madison, WI, USA
[6] Consultant, Fusion Nuclear Technology Consulting, Linkenheim, Germany
[7] Institute for a Secure and Sustainable Environment, University of Tennessee, Knoxville, TN, USA
[8] Israel Ministry of Defense, Tel Aviv, Israel (on sabbatical at PPPL)
[9] Consultant, formerly with The Boeing Company, St. Louis, MO, USA

Received 16 January 2011, accepted for publication 21 July 2011
Published 19 August 2011
Online at stacks.iop.org/NF/51/103014

Abstract
A potentially attractive next-step towards fusion commercialization is a pilot plant, i.e. a device ultimately capable of small net electricity production in as compact a facility as possible and in a configuration scalable to a full-size power plant. A key capability for a pilot-plant programme is the production of high neutron fluence enabling fusion nuclear science and technology (FNST) research. It is found that for physics and technology assumptions between those assumed for ITER and nth-of-a-kind fusion power plant, it is possible to provide FNST-relevant neutron wall loading in pilot devices. Thus, it may be possible to utilize a single facility to perform FNST research utilizing reactor-relevant plasma, blanket, coil and auxiliary systems and maintenance schemes while also targeting net electricity production. In this paper three configurations for a pilot plant are considered: the advanced tokamak, spherical tokamak and compact stellarator. A range of configuration issues is considered including: radial build and blanket design, magnet systems, maintenance schemes, tritium consumption and self-sufficiency, physics scenarios and a brief assessment of research needs for the configurations.

(Some figures in this article are in colour only in the electronic version)

1. Introduction

Recent studies in the United States [1], European Union (EU) [2] and Japan [3] have identified scientific and technological gaps that need to be closed to construct and operate a magnetic fusion power plant following ITER. Within the US, a demonstration power plant (a 'Demo') is generally defined as a first-of-a-kind fusion power plant which aims to be the penultimate step to commercialization in magnetic fusion energy (MFE). The mission elements of a first-of-a-kind fusion power plant have been described in the STARLITE study [4] and are briefly summarized as follows:

- Technology and performance: demonstrate the technologies and plasma operating regimes planned for commercial power plants.
- Integration and scalability: demonstrate all systems working as an integrated unit, close to commercial scale ($\approx$75% in P_{electric}).
- Economics: demonstrate cost-competitiveness.
- Safety, licensing, waste disposal, decommissioning: demonstrate that fusion fulfils its promise of safe, clean energy.
- Reliability, maintainability, availability: demonstrate availability competitive with other energy sources, with less than 1 unscheduled shutdown per year.
- Operability: demonstrate ease of operation, with routine emissions below allowable values.

A key question in the development of fusion power is the choice of development path and associated major fusion

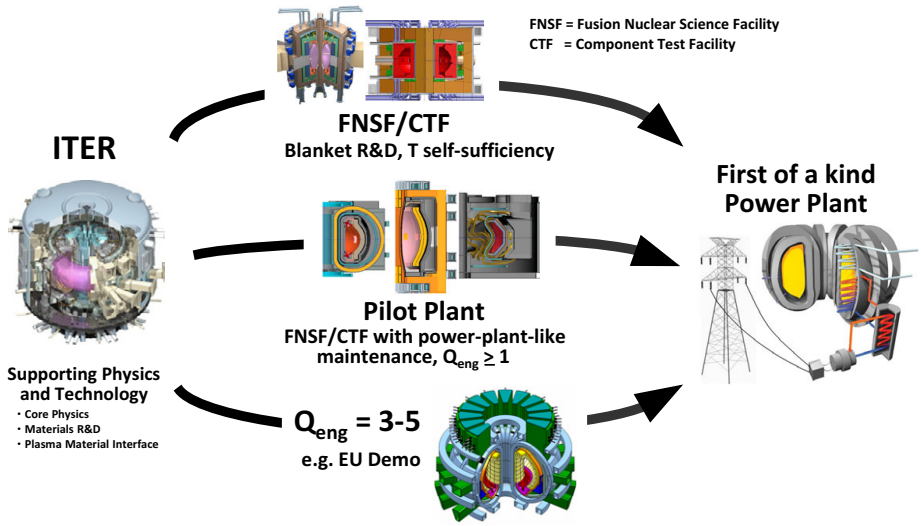

Figure 1. Possible pathways from ITER to a first-of-a-kind fusion power plant.

facility(ies) that can most rapidly and economically close the gaps to a fusion power plant. The fundamental difference between possible paths is the number of mission elements incorporated and the impact of this choice on the required scale and design of any associated facilities. Figure 1 illustrates in a very simplified way several of the possible paths from ITER to a fusion power plant that have been proposed. The major facilities associated with the top-most path in the figure are commonly known as a Fusion Nuclear Science Facility (FNSF) [5], Component Test Facility (CTF) [6] or Fusion Development Facility (FDF) [7]. The FNSF/CTF design concepts have largely been based on a low-aspect-ratio 'spherical' tokamak, whereas the FDF is based on a conventional aspect ratio tokamak. The primary mission element of the FNSF/CTF/FDF path is most closely aligned with the Demo 'Technology and Performance' goal—in particular the development of fusion blanket technology for tritium breeding and power conversion. Both the low and conventional aspect ratio design concepts utilize demountable copper TF magnets for maintainability of the internal components with as compact a design as possible to maximize the neutron wall loading per unit fusion power and T consumption. Achieving tritium self-sufficiency is a very significant hurdle for magnetic fusion and is a primary goal of this path while also enabling access to high-performance plasma scenarios.

Another possible path is to integrate a larger number of mission elements into a facility following ITER and with size and fusion power approaching a full-scale fusion power plant. Such a path is shown at the bottom of figure 1 and would attempt to address many if not all of the STARLITE mission goals. A key difference between this path and the FNSF/CTF/FDF path is increased emphasis on power-plant-relevant magnets and design and technology for integration, scalability and for maintainability. An example design concept on this path is the EU Demo configuration [2, 8]. Analogous studies in Japan [9] have proposed facilities that utilize a development path of phased operational and engineering upgrades in a device larger than ITER to target electricity break-even at $P_{\text{fusion}} \approx 1$ GW during initial operation and ultimately targeting higher fusion power ($P_{\text{fusion}} \approx 3$ GW) and net electricity production at the 0.5–1 GWe level. Economics clearly plays a prominent role in this more encompassing path which has a high ratio of electrical power produced to electrical power consumed $= Q_{\text{eng}} = 3$–5 and a goal of electricity production at the GWe-level.

A third potentially attractive path is that of a pilot plant [10, 11], i.e. a device capable of performing the FNSF/CTF/FDF mission while also incorporating design features projected to enable production of a small amount of net electricity. Further, this 'FNSF-Pilot' path would be designed to be directly scalable to a power plant and would also be as small as possible to reduce device cost and risk. The overall pilot-plant goal is to integrate key science and technology capabilities of a fusion power plant in a next-step R&D facility. The targeted ultimate capabilities include

- Fusion nuclear science and technology development and component testing including steady-state operating scenarios, neutron wall loading $\geqslant 1$ MW m^{-2}, and tritium self-sufficiency.
- Maintenance schemes applicable to power plant, including demonstration of methods for fast replacement of in-vessel components.
- Net electricity production.

The integration of these capabilities while targeting electricity break-even $Q_{\text{eng}} = 1$ with $P_{\text{fusion}} = 0.3$–0.6 GW rather than power-plant scale power production $P_{\text{fusion}} = 2$–5 GW could accelerate the commercialization of magnetic fusion by reducing device size, cost and risk while narrowing or closing most gaps to a first-of-a-kind power plant.

The FNSF-Pilot plant path is shown pictorially in the middle of figure 1 and includes the three configurations studied in this paper: the advanced tokamak (AT), spherical tokamak (ST) and compact stellarator (CS). These configurations are considered because the tokamak currently has the most well-developed physics basis, the ST offers the potential for simplified maintenance, and the CS offers disruption-free operation with low recirculating power. Overall, initial analysis indicates that the CS and AT are the most energy efficient electrically. Compared with the ARIES [12] series

of power-plant designs, preliminary scaling studies indicate that with similar engineering assumptions, the fusion power in a pilot plant with small net electricity production is approximately 20–30% of that of a power plant sized to produce 1 GWe, and the major radius and neutron wall loading are approximately 0.6 times that of a full-scale power plant. Substantial peak outboard neutron wall loading of 2–5 MW m^{-2} is achievable in the pilot plants studied indicating such devices are indeed suitable for consideration as FNST development devices [13]. The pilot-plant devices investigated here are approximately 1.5 times larger in linear dimension than proposed ST [6, 5] and tokamak [7] facilities designed to achieve similar neutron wall loadings but without consideration of electricity production or extrapolation of the configuration to a power plant. The analysis, design and mission considerations for pilot plants are described below. Section 2 discusses engineering efficiency analysis, section 3 assesses device size, section 4 describes the device radial builds based on 1D neutronics analysis, section 5 describes the applicability of pilot plants to fusion nuclear science and technology R&D, section 6 describes remaining research needs for the pilot path and section 7 provides a summary.

2. Engineering efficiency analysis

The overall pilot plant engineering efficiency $Q_{\rm eng}$ is defined as the ratio of electrical power produced to electrical power consumed and can be expressed as

$$Q_{\rm eng} = \frac{\eta_{\rm th}\eta_{\rm aux}Q(4M_{\rm n}+1+5/Q+5P_{\rm pump}/P_{\rm fus})}{5(1+\eta_{\rm aux}Q(P_{\rm pump}+P_{\rm sub}+P_{\rm coils}+P_{\rm control})/P_{\rm fus})} \quad (1)$$

where $\eta_{\rm th}$ is the thermal conversion efficiency, $\eta_{\rm aux}$ is the auxiliary power wall-plug efficiency, $P_{\rm fus}$ is total DT fusion power, $P_{\rm aux}$ is auxiliary power for heating and current-drive, $Q = P_{\rm fus}/P_{\rm aux}$, $M_{\rm n}$ is the neutron energy multiplier, $P_{\rm th} = M_{\rm n}P_{\rm n} + P_{\alpha} + P_{\rm aux}$ is the thermal power, $P_{\rm pump}$ is the coolant pumping power, $P_{\rm sub}$ is the subsystems power, $P_{\rm coils}$ is the power lost in normally conducting coils and $P_{\rm control}$ is the power used in plasma or plant control that is not included in $P_{\rm aux}$. Equation (1) illustrates that the leading terms in the engineering efficiency $Q_{\rm eng}$ involve a combination of technology and physics performance metrics. In particular, $Q_{\rm eng}$ is proportional to the thermal conversion efficiency $\eta_{\rm th}$ and also increases with increasing auxiliary system wall-plug efficiency $\eta_{\rm aux}$ and fusion gain Q. In this analysis, the value of $\eta_{\rm th}$ is varied to assess the impact on device size, a constant $\eta_{\rm aux} = 0.4$ is assumed, the normalized current drive (CD) efficiency $\eta_{\rm CD} = I_{\rm CD}R_0n_{\rm e}/P_{\rm CD} = 0.3\times10^{20}$ A W^{-1} m^{-2} and $M_{\rm n} = 1.1$. The viability of achieving these $\eta_{\rm aux}$ and $\eta_{\rm CD}$ values is discussed further in section 6. The coolant pumping power is relatively small but is included for completeness in the present calculations. The pumping power is assumed to be proportional to the total thermal power: $P_{\rm pump} = 0.03P_{\rm th}$, and it is further assumed that nearly all of the pumping power is due to frictional losses and can therefore be recovered as thermal power. For reference, the ARIES-ST power-plant design required 90 MW of He coolant pumping power (2.6% of the total thermal power) and an estimated 90% of that power was recoverable as thermal power [14]. Similarly, the subsystem + control power is also assumed to be simply proportional to the total thermal power: $P_{\rm sub} + P_{\rm control} = 0.04P_{\rm th}$. Subsystems power includes such things as divertor and main-chamber cryo-pumping power, and control power includes such things as vertical position and resistive wall mode control for the AT/ST. More accurate assessments of the power requirements for these and other auxiliary systems are needed and is a topic for future research.

With the above assumptions, the plasma stability, confinement, magnet technology, tritium breeding ratio (TBR) and shielding requirements to avoid exceeding neutron damage limits together determine the device size needed to achieve $Q_{\rm eng} \geqslant 1$ and support a FNST mission. Other constraints and assumptions for the pilot-plant analysis include

- 20 year pilot-plant lifetime supporting a goal of 10% availability rising to 50% (30% average) = 6 full-power years (FPY).
- Vacuum vessel, manifolds, support structures and superconducting (SC) coils are lifetime components.
- Surface-average neutron wall loading (computed at plasma boundary): $\langle W_{\rm n}\rangle \geqslant 1$ MW m^{-2}.
- Neutron wall load peaking factors (peak/avg): AT/ST/CS = 1.43/1.56/2.0.
- Steady-state operating scenarios with fully non-inductive CD (bootstrap + radio-frequency (RF)/neutral beam injection (NBI) for AT/ST.
- Magnets: SC magnets for the AT and CS, normally conducting toroidal field (TF) and SC poloidal field (PF) coils for the ST.
- Confinement and stability:
  - AT and ST: energy confinement time $\tau_E \propto$ ITER H-mode IPB98(y,2) [15], β at or above the kink no-wall stability limit, $\beta_{\rm N} \leqslant$ present experimental values, and density at or below the Greenwald limit [16].
  - CS: energy confinement time $\tau_E \propto$ stellarator L-mode: ISS04 [17], $\beta \leqslant 7\%$ (based on ARIES-CS analysis), and quasi-axisymmetric (QAS) configuration for tokamak-like confinement, but with higher density and lower temperature.

In the availability assumption listed above, it is implicitly assumed that if 50% availability could be demonstrated in the pilot-plant programme, that would be sufficient to support construction of the first commercial fusion power plant. Additionally, unless otherwise stated, neutron fluxes and wall loadings quoted in this paper are computed at the plasma boundary, i.e. are the ratios of fusion neutron power to plasma boundary surface area.

3. Assessment of device size

An important constraint on overall device size for the AT and CS is the maximum magnetic field strength allowed at the SC TF coil, or equivalently the effective TF current density as determined by SC strand current density and the space needed for magnet cooling, quench protection and structural support. To minimize device size, the AT and CS devices discussed here use effective TF current densities $\langle J_{\rm TF}\rangle \approx$ 20–25 MA m^{-2} and maximum toroidal fields $B_{\rm TF\text{-}max} \approx$ 13–14 T above ITER values (11–12 MA m^{-2} [18], $B_{\rm TF\text{-}max} = 11.8$ T [19, 18]) and

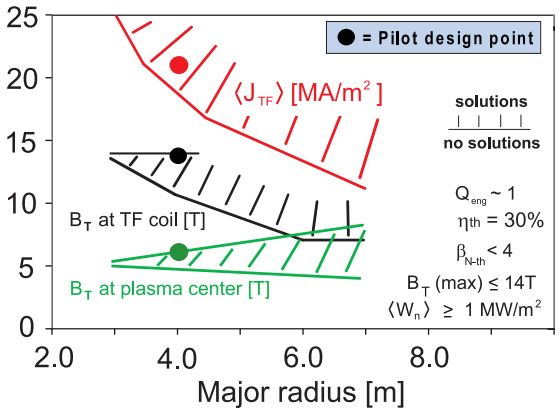

Figure 2. AT pilot $\langle J_{TF}\rangle$ and B_T at TF coil and plasma centre versus major radius.

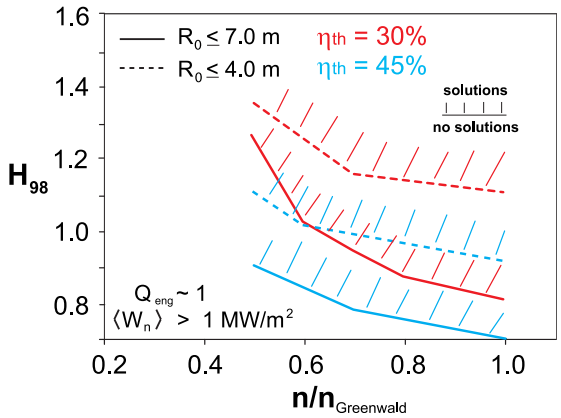

Figure 3. AT confinement multiplier H_{98} required for $Q_{eng} \approx 1$ versus density, R_0 and η_{th}.

will therefore require advancements in SC TF coil technology and/or design. The limits on SC TF coil effective current density are driven primarily by structural limits. Possible ways to increase the effective inboard TF current density include [20]

- Alternative structural concepts, for example bucking versus wedging.
- Increased allowable stress via reduced cycling of the magnets.
- Increased structural fraction by improvements in the conductor, such as improved SC properties, quench detection schemes resulting in decreased Cu requirements and decreased He cooling requirements.
- Grading of the conductor.

Preliminary estimates indicate that the combined effects of these improvements could increase the effective TF current density by a factor up to 1.5 [21] (i.e. up to 18 MA m^{-2}) approaching the values considered here for compact AT and CS pilot plants. For the AT and CS pilot design concepts, an inboard thickness of 1–1.3 m was assumed for the first-wall + blanket + skeleton-ring + vacuum-vessel. This inboard shielding assumption is supported by 1D neutronics analysis described in section 4. Here, 'skeleton ring' [22] refers to an integrated support and shielding structure comprised of shield modules and manifolds to which blanket modules are attached. The skeleton-ring structure is utilized to mechanically and thermally separate the elevated-temperature core components from the colder vacuum vessel in order to withstand large loads caused by gravity, plasma disruptions and thermal expansion.

Figure 2 shows the aspect ratio $A = 4$ AT pilot design space for $Q_{eng} \approx 1$, $\eta_{th} = 0.3$, thermal β_N (i.e. not including fast ions) $= \beta_{N\text{-}th} \leqslant 4$, B_{max} at the TF coil $\leqslant$14 T, and average neutron wall loading $\langle W_n\rangle \geqslant 1$ MW m^{-2}. As shown in the figure, devices with major radius $R_0 \geqslant 3.5$ m at $B_T \approx 5$–6 T are possible. However, with ITER-like TF magnet parameters the pilot size increases to $R_0 \approx 6$–7 m. This trend illustrates the strong sensitivity of the AT pilot device size to the inboard TF effective current density.

Figure 3 shows the dependence of the required confinement multiplier H_{98} on density, device size and blanket thermal conversion efficiency for the AT pilot. A $R_0 \leqslant 4$ m AT pilot requires H_{98} as low as 0.9 at Greenwald fraction $n/n_{Greenwald}$ near 1 for $\eta_{th} = 0.45$, while H_{98} increases to 1.4 at lower $n/n_{Greenwald} \approx 0.5$ for $\eta_{th} = 0.3$. The variation of H_{98} with density is a result of the density dependence of the ITER H-mode confinement scaling, the temperature dependence of the fusion cross-section, and the reduction of CD efficiency at increased density (similar trends are observed for the ST as shown in figure 4). Figure 3 also shows that for larger $R_0 \leqslant 7$ m AT pilots, sub-ITER H-mode confinement multiplier H_{98} of only 0.7–0.9 is needed for $n/n_{Greenwald} = 0.5$ to 1 for $\eta_{th} = 0.45$. There is a stronger dependence on density at lower $\eta_{th} = 0.3$, with H_{98} increasing from 0.8 to 1.3 as $n/n_{Greenwald}$ is lowered from 1 to 0.5.

For an ST pilot it is important to minimize TF resistive losses to 150–200 MW to enable access to $Q_{eng} \approx 1$. To achieve this, the vacuum toroidal field at the plasma geometric centre is limited to $B_T \leqslant 2.4$ T, a flared TF copper centre-post and large cross-section copper TF return legs are utilized. SC PF coils (like ARIES-ST) are used for those PF coils not attached to the centre-post. The ST utilizes a 0.10 m thick shield to reduce radiation damage and nuclear heating of the centre-post Cu TF magnet. The plasma aspect ratio $A = 1.7$.

The ST pilot operating points with $Q_{eng} = 1$ and $\eta_{th} = 0.45$ depend strongly on the normalized density $n/n_{Greenwald}$ as shown in figure 4 for two major radii: $R_0 = 1.6$ and 2.2 m. Negative neutral beam injection (NNBI) heating and CD with injection energy = 0.5 MeV is assumed for the ST pilot. Figure 4(a) shows that at fixed $P_{NBI} = 30$ MW and fixed fusion power, the β_N decreases by $\approx$1 unit for each 0.6 m increase in major radius across the range of Greenwald fractions. This trend is also found for a wider range of major radii than documented here. These β_N values are above the no-wall limit, and resistive wall mode stabilization would be utilized [23]. Figure 4(a) also shows that β_N increases substantially at low density, whereas β_N varies only weakly with density for $n/n_{Greenwald} > 0.6$. Much of the increase in β_N at low density is due to increased fast-ion (NBI + alpha) stored energy fraction (due to increased slowing down time) as shown in figure 4(c). Figure 4(b) shows that the required H_{98} decreases rapidly with increased density as device size is increased and is almost independent of device size at fixed P_{NBI}. Figure 4(d) shows the strong increase in bootstrap fraction with increased density as the NBI-CD decreases at high density. Doubling the heating power at fixed $R_0 = 2.2$ m from $P_{NBI} = 30$ MW (blue) to $P_{NBI} = 60$ MW (black) reduces

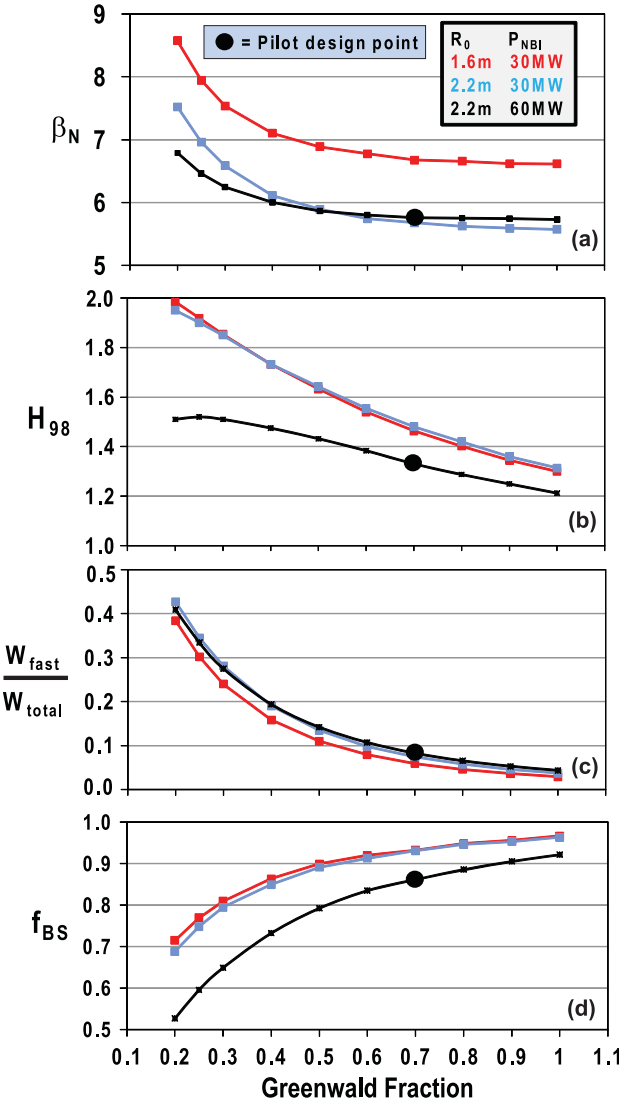

Figure 4. ST pilot β_N, H_{98}, W_{fast}/W_{tot} and f_{BS} versus density at $Q_{eng} = 1$.

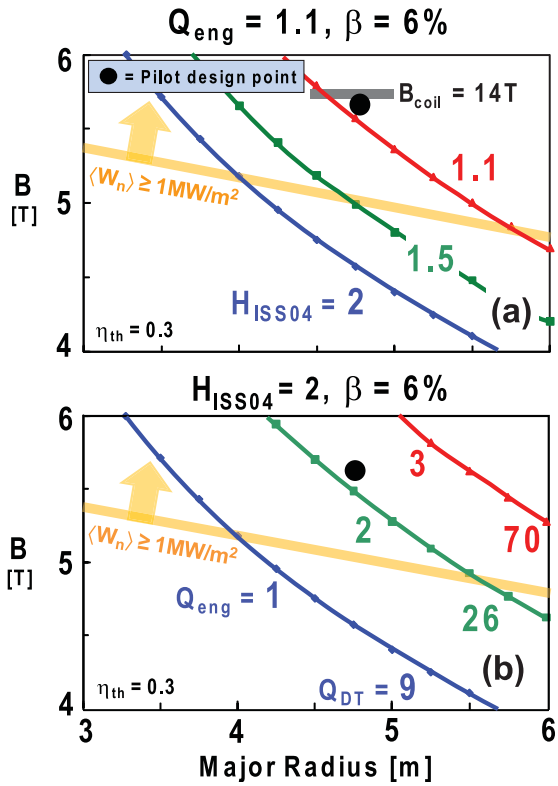

Figure 5. Toroidal field required in the CS pilot versus average major radius for a range of (*a*) H_{ISS04} and (*b*) Q_{eng} values.

the required H_{98} by a factor of 1.1–1.25 and increases the externally controlled NBI-CD fraction by a factor of 1.6–2.

Unlike the AT or ST, the CS pilot does not require auxiliary CD and also has a much wider operating space with respect to plasma density. It is also possible to operate with comparatively low auxiliary power and higher fusion gain Q. The CS pilot device size is therefore largely determined by the achievable magnetic field, confinement and stability. As shown in figure 5(*a*), CS pilots with $B_T \geqslant 5$ T and average major radius $\geqslant$4 m can produce $Q_{eng} > 1$ provided the confinement is near H-mode levels (assumed to be $\leqslant 2\times$ the 2004 international stellarator scaling for L-mode = ISS04) and the total β is near $\leqslant$7% which is assumed to be no-wall stable based on stability analysis for ARIES-CS [12]. Figure 5(*b*) shows that for reduced $H_{ISS04} \approx 1.25$–1.5, increased $B_T \geqslant 6$ T and average major radius $\geqslant$5 m are required to produce $Q_{eng} > 1$.

Based on the analysis above, table 1 summarizes the parameters of pilot devices based on the AT, ST and CS for two values of thermal efficiency $\eta_{th} = 0.3$ and 0.45. This range of thermal efficiencies is chosen to approximately span the range expected for candidate pilot-plant blankets including He-cooled pebble-bed (HCPB) ceramic blankets and dual-coolant breeding blankets with flowing Pb–Li (DCLL) [2, 12, 24, 25]. Several noteworthy trends are evident from table 1. First, the AT pilot plant with $\eta_{th} = 0.45$, $\langle J_{TF}\rangle \approx 21$ MA m^{-2} ($B_{max} = 13$ T) and $Q_{eng} = 1$ has toroidal field, plasma current, β_N and fusion power similar to proposed ITER fully non-inductive scenarios but with reduced $H_{98} = 1.2$ (versus 1.5–1.7 for ITER fully non-inductive scenarios [26–28]) and in a device 30% smaller in major radius. The ability to achieve similar fusion performance in a smaller device results from assumed improvements in TF magnet technology and from sizing the central solenoid to provide only enough flux-swing for plasma current ramp-up. Operation at lower $\eta_{th} = 0.3$ requires higher values of P_{fus}, Q_{DT}, H_{98} and β_N at or above the no-wall stability limit. For comparison, due to inboard space constraints, the ST pilot (like other $A < 2$ designs) has no inboard blanket or solenoid and utilizes single-turn normally conducting (Cu) TF coils. The use of Cu TF coils increases the recirculating power and thus the fusion power required to achieve $Q_{eng} = 1$. As shown in table 1, the ST fusion powers are 1.3–1.5$\times$ the AT values with similar dependence on η_{th}. The ST pilot-plant plasma current is 2.5$\times$ higher than in the AT, and the bootstrap fractions are also higher, although comparable bootstrap current fraction $f_{BS} \approx 0.6$ is achievable in the ST at lower $n_e/n_{Greenwald} = 0.3$ and higher $H_{98} = 1.5$. The ST pilot plasma has the highest average neutron wall loading (due to higher required fusion power) of all configurations assessed with average wall loading $\langle W_n\rangle$ comparable to those previously proposed for nuclear component testing [6]. Finally, for the stellarator pilot plant, to minimize device size, increase neutron

Table 1. Parameters for AT, ST and CS pilot plants for thermal efficiency $\eta_{th} = 0.3$ and 0.45. Parameters for the corresponding full-scale Demo power plants based on scaling pilot plant linear dimensions by a factor of 1.5 are shown in italics.

	AT Pilot	AT Pilot	*AT Demo*	ST Pilot	ST Pilot	*ST Demo*	CS Pilot	CS Pilot	*CS Demo*
η_{th}	0.30	0.45	*0.45 0.59*	0.30	0.45	*0.45 0.59*	0.30	0.45	*0.45 0.59*
$A = R_0 / a$	4.0	4.0	*4.0*	1.7	1.7	*1.7*	4.5	4.5	*4.5*
R_0 [m]	4.0	4.0	*6.0*	2.2	2.2	*3.2*	4.75	4.75	*7.1*
κ	2.0	2.0	*2.0*	3.3	3.3	*3.3*	1.8	1.8	*1.8*
B_T [T]	6.0	6.0	*6.0*	2.4	2.4	*2.4*	5.6	5.6	*5.7*
I_P [MA]	7.7	7.7	*11.6*	20	18	*26.2*	2.1	1.7	*3.3*
q_{95}	3.8	3.8	*3.8*	7.3	7.8	*7.8*	1.5	1.5	*1.5*
q_{cyl}	2.4	2.4	*2.4*	2.8	3.0	*3.0*	-	-	-
f_{BS} or iota from BS	0.69	0.57	*0.71*	0.90	0.86	*0.9*	0.23	0.19	*0.24*
$n_e / n_{Greenwald}$	1	0.9	*0.9*	0.7	0.7	*0.8*	-	-	-
H_{98} or H_{ISS04}	1.22	1.13	*1.14*	1.35	1.34	*1.23*	1.75	1.60	*1.11*
β_T [%]	4.8	4.1	*5.2*	39	31	*35*	6.9	5.7	*6.8*
β_N	3.7	3.2	*4.0*	6.1	5.3	*6.0*	-	-	-
P_{fus} [MW]	674	510	*2077*	1016	645	*2290*	529	313	*1794*
P_{aux} [MW]	79	100	*100*	50	60	*60*	12	18	*18*
Q_{DT}	8.5	5.1	*20.8*	20.3	10.8	*38.2*	44	17	*100*
Q_{eng}	1.0	1.0	*2.6 3.4*	1.0	1.0	*2.2 2.8*	2.5	2.4	*5.0 6.5*
Net Electric [MW]	0	0	*670 1000*	0	0	*630 1000*	110	95	*725 1000*
$<W_n>$ [MW/m^2]	2.2	1.7	*3.0*	3.1	2.0	*3.4*	1.8	1.1	*2.8*
Peak W_n [MW/m^2]	3.1	2.4	*4.3*	4.9	3.1	*5.2*	3.6	2.2	*5.6*
$P_{alpha+aux}$ / R [MW/m]	53	50	*86*	115	86	*161*	25	17	*53*
$P_{alpha+aux}$ / S [MW/m^2]	0.87	0.82	*0.93*	0.98	0.73	*0.94*	0.52	0.35	*0.72*

wall loading for FNST, and utilize physics assumptions closest to the AT, a QAS CS design with low average aspect ratio $\langle R_0/a \rangle = 4.5$ is chosen. Favourably, for $\eta_{th} = 0.3$, the CS has fusion power 500 MW; similar to the AT but with much lower P_{aux}, 3–5× higher Q_{DT}, and $Q_{eng} = 2.5$ due to elimination of external CD power and the usage of H-mode like confinement ($H_{ISS04} = 1.75$). Higher η_{th} enables solutions with similar Q_{eng} at lower $P_{fus} \approx 300$ MW.

Lastly, an important consideration for the pilot-plant approach to fusion development is the degree of extrapolation in physics and engineering performance required beyond simply scaling the physical dimensions of the pilot plant to the full-size first-of-a-kind fusion power plant. To address this, table 1 also contains parameters for three representative AT, ST and CS 'Demo' configurations where the pilot-plant major radius has been increased by a factor of 1.5 and other performance parameters have been adjusted to achieve a net electric power output of approximately 600–700 MWe for $\eta_{th} = 0.45$ and a net electric power output of 1 GWe for $\eta_{th} = 0.59$ as utilized in the ARIES-AT power-plant design [12]. As is evident from table 1, the plasma shape, magnetic field, safety factor, bootstrap current fractions, normalized density, confinement enhancement factors and beta values change relatively little in the scale-up from pilot plant to full-scale power plant. However, the fusion gain Q_{DT} approximately doubles, the neutron wall loading increases as much as 50%,

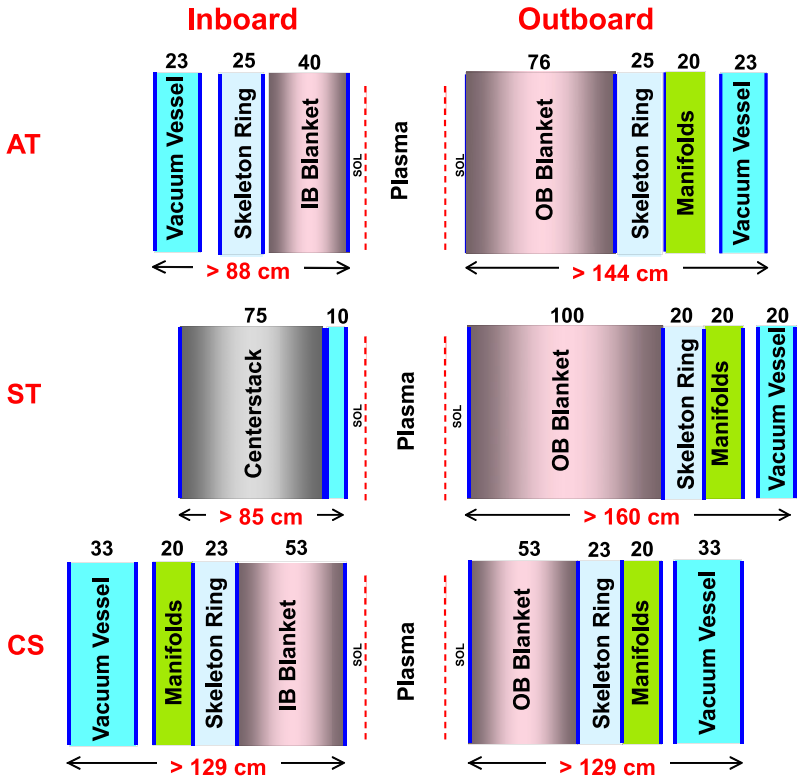

Figure 6. Radial builds of pilot blankets, skeleton rings, manifolds and vacuum vessels.

and the divertor heat-flux parameter P/R increases by a factor of 1.5–2 in the scale-up to Demo. Thus, the largest extrapolations in scaling from pilot plant to full-scale power plant appear to be in the degree of plasma self-heating and in the divertor power handling and blanket power extraction technologies.

4. Radial build, device layout and maintenance

A critical aspect of pilot design is provision for adequate space for internal components including breeding blankets, neutron shielding, structural supports and manifolds. The parameters summarized in table 1 combined with lifetime assumptions and maintenance requirements enable estimation of the radial build requirements for each pilot-plant configuration. The pilot-plant lifetime is assumed to be 20 years with availability 10% increasing to 50% (30% average) = 6 FPY. The vacuum vessel, manifolds, skeleton rings and SC TF coils are assumed to be lifetime components as are the normally conducting TF coils for the ST (with the exception of the centre-post). Damage to ferritic steel (FS) structure is limited to 80 dpa, and He production is limited to 1 He appm where reweldability is required. For the SC magnets (operating at 4 K), the peak fast neutron fluence to Nb_3Sn ($E_n > 0.1$ MeV) is limited to 10^{19} n cm^{-2}, peak nuclear heating $\leqslant 2$ mW cm^{-3}, peak dpa to Cu stabilizer $\leqslant 6 \times 10^{-3}$ dpa, and peak dose to electric insulator $\leqslant 10^{10}$ rad. Finally, the overall TBR for all blanket systems is required to be approximately 1.1 in order to achieve net TBR of 1.01 including TBR reductions from test modules and/or large penetrations.

Preliminary inboard and outboard radial builds for DCLL blankets for the AT, ST, and CS pilots are shown in figure 6 based on these specifications. For the purposes of computing a lower bound on FPY before nuclear component replacement is required (i.e. an upper-bound on the expected neutron fluence), the parameters corresponding to the lower thermal conversion efficiency $\eta_{th} = 0.3$ in table 1 are used. Further, it is assumed that the surface area of the first-wall is 1.2× the surface area of the plasma boundary. For all three configurations, this corresponds to having a gap of approximately 0.1 m between the plasma boundary and the first-wall. As discussed in section 6, this distance is much larger than the expected characteristic scrape-off layer (SOL) widths in the pilot plants. However, ELMs and/or filamentary structures will also be present in the SOL and may enhance the plasma–wall interactions unfavourably [29]. Additional distance between the plasma and outer wall could be added to the pilot-plant radial build with only a modest increase in overall device size; however, this increased distance would reduce the achievable neutron wall loading for the FNSF mission. For the AT, an inboard (IB) blanket thickness of 40 cm is used and would be replaced every 2.5 FPY. The OB blanket would be 76 cm thick, and would also be replaced every 2.5 FPY. For the ST, on the inboard side, there is a 10 cm thick He-cooled FS shield + vacuum vessel to reduce nuclear heating and radiation damage of the Cu magnet. It should be noted that other coolants (water and heavy water) and shielding materials (W, WC, WB, SiC, Be, C, V) have previously been examined as possible coolant+inboard shield combinations for the ST, but He-cooled FS offers the best overall performance taking into account shielding effectiveness, ability to recover high-grade heat, and

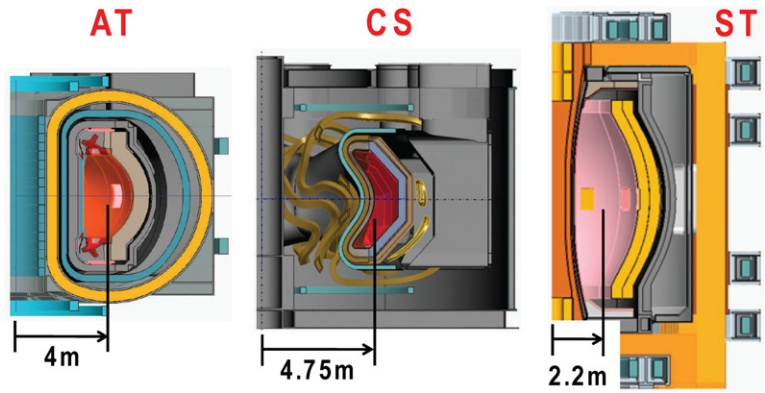

Figure 7. Pilot plant elevation views and radial dimensions for the three configurations.

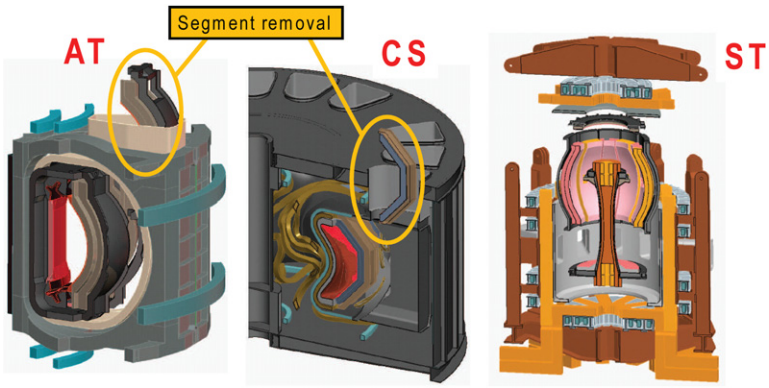

Figure 8. Pilot plant 3D views of vertical maintenance schemes.

impact on TBR [14]. The combined radial build of the TF Cu conductor plus shield + vacuum vessel is 0.85 m at the vertical midplane, and the radius of TF Cu conductor increases above and below the midplane (i.e. the conductor is flared to minimize resistive power losses) as shown in figure 7. Because of the higher neutron wall loading in the ST, the inboard midplane shielding structure would require replacement every 1.8 FPY, and the central Cu TF magnet would be replaced concurrently. The Cu of the ST centre-post TF coil becomes embrittled at 0.1 dpa (2–3 days of full-power operation), but central TF conductor designs are possible that keep stresses below allowable limits [30]. On the outboard side, a 1 m thick blanket is used and would require replacement every 1.4 FPY. Finally, for the CS, a uniform 53 cm thick blanket is used everywhere except behind the divertor and would require replacement every 2.3 FPY.

Based on the pilot parameters in table 1 and radial build information in figure 6, 3D conceptual designs have been developed for each configuration incorporating free-boundary equilibrium calculations and conventional divertor designs for the AT and ST. The AT design incorporates a central solenoid sufficient for plasma current ramp-up, whereas the ST requires solenoid-free ramp-up using NBI and bootstrap CD. A side-by-side and to-scale comparison of all three configurations is provided in figure 7.

Special attention has been paid to device maintenance, and a vertical maintenance scheme has been initially adopted for each of the pilot configurations. As shown in figure 8, for the AT, individual toroidal segments are translated radially or toroidally then radially, then lifted vertically through ports above the pilot core. For the CS, the modular coils have been straightened in the outboard sections (not yet re-optimized to satisfy plasma requirements) enabling the incorporation of vertical ports similar in design to the AT. Design strategies to simultaneously satisfy physics requirements and criteria for favourable maintenance are being investigated [31]. As shown in figure 8, CS individual toroidal segments are also translated radially or toroidally then radially, then lifted vertically through the ports above the pilot core. For the ST, the upper support structure, PF coils and TF horizontal legs are removed as a unit, and then the core (centre-post + blankets + skeleton) is removed vertically either as a unit or in a small number of components.

To provide an example of a more detailed assessment of pilot-plant maintenance, the in-vessel component segmentation for an AT pilot plant with 12 toroidal field coils is shown in figure 9. For this maintenance concept, inboard blanket-shield modules are separated from outboard blanket-shield modules and outboard blanket-shield posts. The inboard and outboard blanket-shield modules are toroidally centred between TF coils and can be removed by translating radially then lifting vertically through maintenance ports above the pilot core as shown in figure 8. The outboard blanket-shield posts are toroidally centred at the TF coils and can be removed by translating toroidally, then radially, then lifting vertically. Thus there is one inboard blanket-shield segment per TF sector and two outboard blanket-shield segments per TF sector for a total of three segments per TF sector. The divertor modules may have a shorter lifetime than the blanket-shield-support structures,

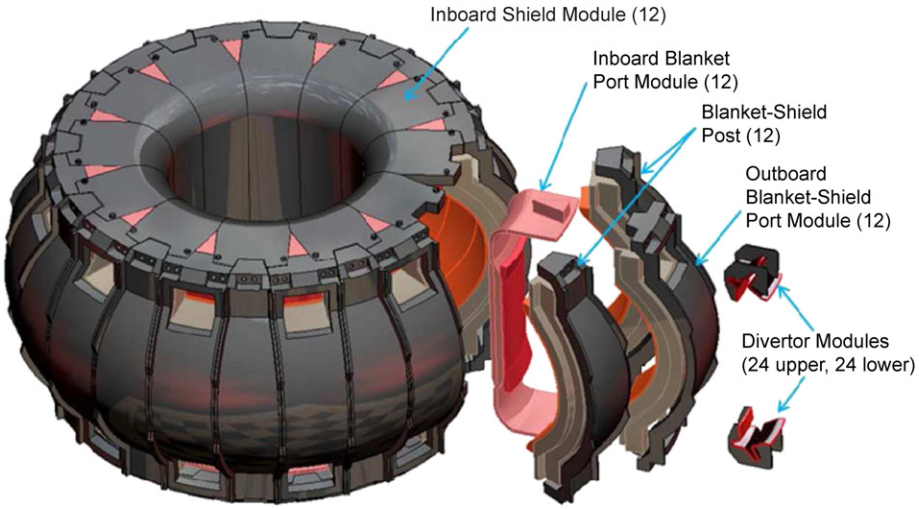

Figure 9. AT pilot plant vertical maintenance concept showing segmentation details of the in-vessel components.

and it is therefore likely beneficial to have replaceable divertor modules. The divertor system is therefore comprised of independent modules which are radially then vertically retractable from the top and bottom of each outboard blanket-shield module and post. There are therefore four divertor modules per TF sector.

The overall number of major in-vessel components for the AT maintenance concept described above is 96 assuming 12 TF coils. This number of components is comparable to that proposed in the 'multi-module' concept [32] of the EU Demo which also utilizes vertical maintenance. Component counts in this range may be a reasonable compromise between the desire to reduce the number of large components (to increase scheduled availability) and decreasing the component size (which increases the component count) to reduce electromagnetic loads from disruptions and to better accomodate thermal expansion. For all of the pilot plants, substantial additional engineering and design is needed to further develop maintenance strategies and to enable detailed comparisons between possible maintenance approaches.

5. Applicability of pilot plants to FNST development

5.1. Tritium consumption

The pilot plants described here are projected to produce 0.3–1 GW fusion power to achieve $Q_{\rm eng} \geqslant 1$. Since the DT fusion T burn-up rate is 56 kg/GW-y, full-power pilots would consume 17–56 kg of T per FPY. The total T consumption of the pilot plant for 6 FPY is therefore 102–336 kg. The world maximum T supply (from CANDU) over the next 30–40 years is 25–30 kg, and ITER is projected to consume nearly all of this amount assuming 0.5 GW fusion power operation at 2% duty factor for 10 years and including T decay at 5.5% per year. Thus, blanket technology development programmes aiming to achieve T self-sufficiency would have available at most approximately 0–5 kg of T. If no T was available at the beginning of pilot operation, the pilot programme would have to purchase T from external sources at an estimated cost of 30–100 M USD/kg. Thus, it is highly advantageous if not imperative that a pilot plant achieve tritium self-sufficiency early in its operational lifetime.

The requirements and strategy for establishing the feasibility, operability, and reliability of blanket and plasma-facing-component (PFC) systems has been established over several decades [13]. The fusion testing requirements for blanket development include local neutron wall loading $\geqslant$1 MW m^{-2}, steady-state operation, test area $\geqslant$10 m^2 and testing volume $\geqslant$5 m^3. The development programme is envisioned to have three phases: (I) fusion break-in for initial exploration of performance in a fusion environment with neutron fluence of 0.3 MW-y m^{-2}, (II) engineering feasibility phase for concept performance verification and selection with 1–3 MW-y m^{-2} and (III) engineering development and reliability growth with $\geqslant$4–6 MW-y m^{-2} accumulated test-time utilizing multiple improved blanket versions.

All three pilots have sufficient outboard testing surface area and volume to incorporate test blanket modules. The AT and ST pilots require a fusion power of roughly 200 MW to produce a peak outboard neutron wall loading of 1 MW m^{-2}, while a CS (due to the 3D dependence of the neutron production rate) would require $\approx$150 MW of fusion power. Thus, to complete phase III of the blanket development programme with 6 MW-y m^{-2} (peak) would require 45–72 kg of T, which clearly requires TBR $\approx$1 given the expected availability of T. Thus, it is expected tritium breeding blankets will need to be installed behind all available plasma facing surfaces (excepting divertor regions) no later than the middle to end of phase I of pilot operation. However, there is a reasonable margin for breeding uncertainty for the pilots, since even a 10% reduction in achievable breeding (TBR $\geqslant$ 0.9) would require only 5–7 kg of T to complete phase III. Thus, it should be possible to establish the engineering feasibility of blanket systems during initial pilot-plant operation. Further, assuming TBR = 1 is established during phase I of operation, it should be possible to extend operation to higher fluence in phases II and III of development without requiring additional T from external sources. Smaller FNST devices [5–7] designed specifically to maximize neutron wall loading per unit fusion power will consume less T per MW-y m^{-2} than a pilot, but will

nevertheless also need to breed or purchase T during phase II of the blanket development programme.

5.2. Fusion performance requirements

An important characteristic of the pilot plants described here is that lower-fusion-performance and therefore less demanding operating scenarios are accessible in the pilots which remain relevant to FNST. In particular, pilot operating scenarios with peak neutron wall loading of 1 MW m^{-2} (to begin a blanket development and testing programme) exist with core plasma confinement and stability comparable to what has already been achieved in existing experiments. As described above, for the AT/ST/CS, peak outboard neutron wall loading $\approx$1 MW m^{-2} corresponds to $P_{\rm fusion} \approx 200/200/150$ MW (assuming the test modules are placed close to the plasma boundary). Starting from the scenarios in table 1, the corresponding plasma parameters to achieve this level of fusion performance in the AT/ST are $\beta_{\rm N} = 2.7/3.9$, $\beta_{\rm t} = 2.8/17\%$, $H_{98} = 1.1/1.3$, $Q_{\rm DT} = 2.5/3.5$, $I_P = 6.1/13.5$ MA and $P_{\rm aux} = 79/60$ MW. These values of $\beta_{\rm N}$ are at or below expected optimized kink no-wall stability limits [33] which could potentially reduce the requirements for active feedback control of resistive wall modes. Further, these values of normalized performance ($\beta_{\rm N}$, $\beta_{\rm t}$, H_{98}) have been experimentally achieved or exceeded for nearly one current redistribution time with high non-inductive CD fraction near 100% in the AT [34] and 65–70% [35–37] in the ST with prospects for increasing the ST non-inductive fraction towards 100% utilizing more tangential NBI injection in upgraded ST devices [38]. A research need for the AT and ST pilots is to achieve this level of performance with fully equilibrated profiles and with low disruptivity. Similarly, FNST development can also be achieved at reduced required fusion performance in a CS pilot with peak neutron wall loading of 1 MW m^{-2} with parameters $\beta = 3.6\%$, $H_{\rm ISS} = 1.5$, $Q_{\rm DT} = 3.5$ and $P_{\rm aux} = 45$ MW. This level of normalized performance (β, $H_{\rm ISS}$) has largely been achieved in higher aspect ratio stellarators operated at reduced toroidal magnetic field 0.5 T to assist in the achievement of high beta of up to 4% [39] and/or by utilizing high-density operation and a divertor with partial detachment to achieve a sustained high-confinement H-modes [40]. A research need for a CS pilot is to extend/validate this level of performance to lower aspect ratio and collisionality in the QAS configuration.

5.3. Maintenance approach

A key issue to be assessed for the pilot approach to FNST development is the impact of the maintenance scheme on blanket development. The vertical maintenance scheme proposed for the ST pilot is similar to that previously proposed for ST-based FNSF/CTF devices, so the primary difference between the ST-based FNSF and the ST-Pilot is the larger size and mass of the pilot blanket systems. The AT/CS pilots are also larger than the corresponding AT-based FNSF/CTF. Further, the AT and CS pilots utilize SC TF coils which necessitates using a toroidally segmented vertical (or horizontal) maintenance scheme. This is in contrast to the demountable copper coils of FDF which potentially enable removal of much larger segments of the blanket structure.

If the larger mass of the pilot blanket systems and the toroidal segmentation of the AT/CS pilot blankets do not represent a major impediment to blanket development, then the pilot approach could accelerate fusion development by enabling rapid blanket development while also targeting the conditions for net electricity production utilizing maintenance schemes, operating scenarios and supporting technologies that more readily extrapolate to a full-scale power plant.

The choice of maintenance scheme is clearly a critical issue for the pilot plant. Beyond the impact on blanket development, the maintenance scheme will also impact the design of the power core, the size and layout of hot cells, waste processing, and the location of other auxiliary equipment and the required reliability of such equipment. Thus, the overall pilot availability will be influenced by components other than the blanket modules, and this must also be accounted for when striving to design a pilot plant capable of ultimately achieving average availability of 30% and peak availability up to 50%.

6. Research needs

Many research needs remain for the pilot-plant concept. One of the key technology development needs for all configurations is improved magnets. For the SC AT and CS pilots, TF magnets with up to 2$\times$ higher inboard effective current density is required to achieve compact device size. For the ST, the development and fabrication of large single-turn, radiation-tolerant Cu TF magnets is needed. For the CS, additional engineering and physics analysis is needed to assess passive shaping by high-temperature-SC tiles and/or trim coils proposed to simplify CS coils and improve maintainability and availability. For physics needs, the AT and ST require fully non-inductive operation at high elongation operating near or above the $n = 1$ no-wall limit with very low disruptivity. Since external non-inductive CD is required for the AT and ST, high-efficiency non-inductive CD is also needed. The ST additionally requires non-inductive plasma current ramp-up. While both the ST and QAS CS share a substantial physics basis with the conventional aspect ratio tokamak, additional development of the ST and CS physics bases is needed to reduce risks in extrapolation to larger device size.

With regard to non-inductive CD, substantial improvements in physics and/or technology are likely required to achieve the assumed overall efficiency parameter $\eta_{\rm aux} \times \eta_{\rm CD} = 0.12 \times 10^{20}$ A W^{-1} m^{-2}. For example, for the 0.5 MeV NNBI CD for the ST pilot plant, the assumed $\eta_{\rm CD} = 0.3$ is comparable to values obtained using 0D slowing-down calculations [41], and measured NNBI CD efficiencies have previously been shown to agree well with predicted values [42]. However, using the ITER NNBI system design as a reference, the present source efficiency is approximately 0.66, and the transmission efficiency of the accelerated beam through the neutralizer and into the plasma is approximately 0.46, yielding an overall energy efficiency $\eta_{\rm aux} = 0.3$ [43]. Proposed means of increasing the transmission efficiency by increasing the maximum neutralization efficiency of $\approx$60% for gas-based systems include plasma neutralization ($\approx$80% efficient) [44] and laser photo-detachment ($\approx$95% efficient) [45]. Such improvements could increase $\eta_{\rm aux}$ to 0.4 or higher as assumed here for the pilot plants, but require substantial research and

Table 2. Comparison of neutron wall loading and several plasma–material interface (PMI) parameters for ITER, FNSF devices, pilot plants and ARIES-AT power plant.

	ITER	ST-FNSF	ST-CTF	FDF	Pilot-AT η_{th} = 0.3	Pilot-AT η_{th} = 0.45	Pilot-ST η_{th} = 0.3	Pilot-ST η_{th} = 0.45	Pilot-CS η_{th} = 0.3	Pilot-CS η_{th} = 0.45	ARIES-AT
$P_{neutron}$ / S [MW/m^2]	0.6	0.7	1.5	1.6	2.2	1.7	3.1	2.0	1.8	1.1	3.3
$P_{aux+\alpha}$ / S [MW/m^2]	0.2	0.5	1.0	0.9	0.87	0.82	0.98	0.73	0.52	0.35	0.9
$P_{aux+\alpha}$ / R [MW/m]	25	38	73	43	53	50	115	86	25	17	79
$W_{kin+pol}$ / S [MJ/m^2]	0.8	0.3	0.5	0.6	0.7	0.6	1.1	0.9	0.9	0.7	1.4
Log_{10} [exp(2.5I_P [MA])]	16	8.7	13	7.3	8.4	8.4	22	20	2.3	1.8	14

development. For RF-based CD methods, lower hybrid current drive (LHCD) offers high CD efficiency and high $\eta_{CD} = 0.2$–0.3 values have been obtained on a range of devices [46]. However, klystron efficiencies are limited to approximately 50–55% [47], so achieving $\eta_{aux} = 0.4$ with LHCD requires a combined transmission and plasma coupling efficiency no smaller than 75–80%. Achieving this coupling efficiency may prove challenging in the low-density SOL of H-mode plasmas with a large gap between the last-closed-flux-surface and the LHCD launcher. Recent experiments in the JET tokamak have shown that local gas puffing can significantly improve LHCD coupling efficiency [48] in H-modes with large plasma–launcher gaps. However, the measured CD efficiency is not as high (up to 80–85%) as for small plasma–launcher gap, and additional transmission losses are present between the klystron source and the launcher that further decrease overall transmission efficiency. Such gas puffing may also reduce the H-mode confinement performance of the plasma [48]. Thus, further optimization of LHCD efficiency is required.

Another important research need is improved plasma–material interface (PMI) physics and technology development. Table 2 compares neutron wall loading values and several PMI parameters across the range of FNSF and Pilot devices. As seen in the table, all the proposed FNSF/CTF/Pilot devices have average neutron wall loadings 1–2.5 times higher than the ITER level, and the pilot-plant values are at least 2–3 times higher than ITER (pilot values shown correspond to $\eta_{th} = 0.45$ in table 1). The ratio $P_{aux+\alpha}/S =$ the heating power (auxiliary power + alpha power ignoring radiation losses) normalized to the plasma surface area S is a metric of the steady-state first-wall and/or divertor heat-flux challenge. As is evident from the table, the AT and ST FNSF-Pilot $P_{aux+\alpha}/S$ is up to a factor of 2–5 times higher than for ITER. Similarly, the ratio $P_{aux+\alpha}/R$ (where R is the major radius of the plasma geometric centre) is another common metric of the divertor heat-flux challenge and is a factor of 1.5–3 times larger than for ITER. The CS pilot has P/S and P/R values more comparable to ITER due to the larger device size and smaller fusion power relative to the AT and ST pilots.

A key constraint in device design is the need to limit the peak divertor heat flux to values compatible with the temperature limits and heat removal capacity of the divertor PFCs. The leading candidate divertor PFC for future fusion power plants is tungsten due to favourable material properties including: high melting point and thermal conductivity and low activation, thermal expansion and sputtering yield. Challenges of tungsten include high hardness and brittleness which make the fabrication of tungsten components difficult. For the purposes of assessing the pilot-plant divertor, it is assumed here that the heat-flux limit of helium-cooled tungsten is 10 MW m^{-2} [49]. The width of the heat-flux profile in the SOL is another critical parameter in projecting the peak divertor heat flux, since the peak heat flux varies inversely with this width. Multi-machine databases and scalings exhibit a wide variation in predicted outboard midplane SOL heat-flux width λ_q and this variation represents a substantial uncertainty in projecting to future devices including ITER [29]. Recent dedicated multi-machine studies in the US [50–52] have explored the λ_q scaling further and find a strong inverse dependence on plasma current but a weak dependence on magnetic field and power into the SOL. A drift-based model of the SOL width that is consistent with the recent US experiments (and some JET data) has been developed [53] and can be used (with a significant degree of uncertainty) to project to tokamak and ST pilot plant devices. Such scalings remain to be developed for CSs.

For the parameters shown in table 1, the projected $\lambda_q = 1.4/1.6$ mm for the AT pilot plant/Demo, and $\lambda_q = 2.0/2.6$ mm for the ST pilot plant/Demo. It should be noted that the drift-based model [53] scales as $P_{SOL}^{1/8}(1+\kappa^2)^{5/8}a^{17/8}B^{1/4}I_P^{-9/8}R^{-1}$, and that the larger a and κ and smaller R of the ST lead to a larger projected λ_q relative to the AT despite the higher plasma current of the ST. The size scaling of λ_q is arguably now the most uncertain dependence in the present scalings, and remains a critical issue for projecting to larger devices. Using this midplane heat-flux width parameter, the peak heat flux to the outboard divertor can be expressed as

$$Q_{out}^{peak} = \frac{P_{heat}^{SOL}(1-f_{rad})f_{obd}\sin(\theta_{plate})}{2\pi R_{strike}N_{div}f_{exp}\lambda_q} \qquad (2)$$

where P_{heat}^{SOL} is the alpha + auxiliary heating power to the SOL in the absence of radiative losses, f_{rad} is the assumed fraction of radiation, f_{obd} is the fraction of SOL power to the outboard divertor legs, θ_{plate} is the poloidal angle of inclination between the divertor plate and divertor magnetic field lines, R_{strike} is the major radius of the divertor strike-point, N_{div} is the number of divertor strike-points, and f_{exp} is the poloidal flux expansion $= |\nabla\psi|_{midplane}/|\nabla\psi|_{strike}$. The extrapolated Demo devices have the highest projected divertor heat flux, and to limit the peak heat flux to $\leqslant$10 MW m^{-2} the following parameters for the AT and ST are chosen: $f_{rad} = 0.7$, $f_{obd} = 0.8$, $\theta_{plate} = 10^\circ$, $N_{div} = 2$ (i.e. double null operation with assumed 50 : 50 power

split), and $f_{exp} = 20/25$ for the AT/ST. The f_{rad} value is limited to 0.7 to reduce the probability of burn instability and reduce the impact of high radiated power fraction on confinement [54], $f_{obd} = 0.8$ is representative of the outboard power fraction observed in DIII-D double-null discharges [55], $\theta_{plate} = 10^{\circ}$ is a relatively shallow angle of incidence that would require very good plasma shape and position control and divertor tile imbrication and precise alignment to avoid locally exceeding heat-flux limits, and high flux expansion factors $f_{exp} = 20$–25 would be required using novel divertors [56, 57] that have begun to be favourably explored for heat-flux reduction in present devices [58, 59]. It is noted that the projected flux expansion factor required for the ST is 25% higher than for the AT, and that flux expansion factors this high or higher have already been achieved in NSTX using the 'snowflake' divertor [59]. Further increases in flux expansion and/or R_{strike} are possible with the 'Super-X' divertor [56] which is planned to be tested on the MAST Upgrade device. Divertor radiation/detachment is also a possible means to reduce the peak heat load, but it is unclear if this will extrapolate to the pilot plant/Demo regime [54].

Turning now to the issue of disruptions, the ratio $W_{kin+pol}/S$ is the plasma stored energy (thermal + fast-ion kinetic + poloidal field energy from plasma current) normalized to the plasma surface area S is a metric of the maximum energy flux (e.g. from radiation from disruption mitigation) that could be liberated to the first-wall during a rapid disruptive plasma quench. The ST-FNSF/CTF devices have W/S values 1/3 to 2/3 of those of ITER, while the AT, ST and CS pilot values are comparable to ITER. For reference, the AT power-plant concept ARIES-AT has 1.8 times higher W/S than ITER. From these comparisons it is evident that the steady-state power handling of FSNF/Pilot devices is more demanding than ITER, but the disruption energy loads may be similar to ITER. Finally, the formation of large runaway-electron (RE) currents during disruptions is a substantial threat to ITER and potentially the pilot plants. One metric of RE formation is the runaway avalanche gain [60] $\exp(\gamma_{RA}\,\Delta t) \approx \exp(2.5 I_P(\mathrm{MA}))$ where the exponent coefficient 2.5 is approximate and applicable to conventional aspect ratio tokamaks. The AT/ST FNSF/CTF and AT pilot devices have avalanche gains well below the ITER value, but may still be prone to developing substantial runaway current fractions. The ST pilot has the highest plasma current and highest apparent avalanche gain. However, the ST also has up to a factor of two lower plasma inductance due to reduced aspect ratio [61], and therefore likely has similar effective avalanche gain as the AT pilot. Thus, disruption mitigation schemes developed on ITER are potentially applicable to the AT and ST pilot plants as well. The CS pilot has much smaller plasma current and avalanche gain values comparable to present 1–2 MA medium-scale tokamak devices which do not generally suffer from major RE damage.

While the overall steady-state and disruptive power/energy loads may be roughly comparable to ITER values, the expected pulse-lengths and duty factors in FNSF-Pilot devices would far exceed those of ITER, and arguably represent the largest research need to enable a fusion nuclear science and technology programme. To access high neutron fluence over a reasonable duration, high duty factor (10–50% availability goal versus 2% in ITER) is required, and achieving equilibrated testing conditions demands very long pulses up to $\approx 10^6$ s (versus 10^2–10^3 s in ITER). Further, high-temperature first-wall capability (T_{wall} = 350–550 °C, and possibly up to 700 °C) will be needed to assess the thermal performance of fusion blanket systems and achieve the power conversion efficiencies needed for economical electricity production. Disruption avoidance schemes must also therefore be extended to much longer pulse-lengths and higher duty factors of the pilot plants. Further, pilot-plant first-wall and blanket structures must ultimately be able to withstand mitigated disruptions while still remaining compatible with efficient tritium breeding. The development and/or validation of such disruption avoidance and mitigation schemes would necessarily be an integral part of a pilot-plant research programme.

Finally, if a pilot plant is to have an FNST mission and is to extrapolate to a commercial power plant, device maintainability will be paramount. A vertical maintenance scheme is proposed here for all three configurations enabling segment removal and replacement of major internal components (possibly the entire core for the ST). Additional research is needed to assess the advantages and disadvantages of this approach, and to determine approaches for maintaining smaller internal components. These issues will be addressed in future work.

7. Summary

A preliminary systematic comparison of three candidate pilot-plant configurations has been performed. The configurations considered are the advanced tokamak, the spherical tokamak and the compact stellarator. For each configuration, design concepts have been developed that are sized between FNSF/CTF devices and a conventional Demo. These preliminary design concepts incorporate

- 20 year pilot-plant lifetime supporting a goal of 10% availability rising to 50% (30% average) = 6 full power years.
- Vacuum vessel, manifolds, support structures and superconducting magnets as lifetime components.
- Radial builds compatible with nuclear and thermal shielding requirements.
- Sufficient space for blankets for tritium breeding ratio (TBR) = 1.
- Neutron wall loading $\geqslant 1\,\mathrm{MW\,m^{-2}}$ for blanket research and development.
- Average neutron wall loading up to 2–3 $\mathrm{MW\,m^{-2}}$ for accelerated blanket development.
- Vertical maintenance schemes applicable to power plants.
- Device sizing and technology projected to enable small net electricity production to bridge the gap to GWe power-plant devices.

Based on these findings, it may be possible to utilize a single facility to perform FNST research, incorporate power-plant-relevant plasma, blanket, coil and auxiliary systems and maintenance schemes, and also target net electricity production. Importantly, all three configurations can access reduced fusion performance regimes with operating scenarios near those already achieved in existing devices while remaining

relevant to FNST by delivering peak neutron wall loadings of 1 MW m^{-2}. Nevertheless, substantial research needs remain for all FNSF-Pilot devices ranging from magnet development to improved physics and technology capabilities for very long-pulse sustainment, mitigation of high steady-state and transient/disruptive heat loads, and operation with power-plant relevant first-wall and divertor materials and temperatures. Finally, it is apparent that each of the three configurations has potential advantages and disadvantages, and the ultimate solution likely resides in a combination of AT, ST and CS features.

Acknowledgments

This work was supported by the United States Department of Energy under contract number DE-AC02-09CH11466 (PPPL).

References

[1] Research needs for magnetic fusion energy sciences 2009 (http://burningplasma.org/web/ReNeW/ReNeW.report.web2.pdf)
[2] Maisonnier D. *et al* 2007 *Nucl. Fusion* **47** 1524
[3] Tobita K. *et al* 2006 *Fusion Eng. Des.* **81** 1151
[4] Najmabadi F., Tillack M.S. and Waganer L.M. 1995 The STARLITE project: the mission of the fusion demo *16th IEEE Symp. on Fusion Engineering (Champaign, IL, 1995)* http://www-ferp.ucsd.edu/NAJMABADI/PAPER/95-IEEE.pdf
[5] Peng Y.-K.M. *et al* 2009 *Fusion Sci. Technol.* **56** 957
[6] Peng Y.-K.M. *et al* 2005 *Plasma Phys. Control. Fusion* **47** B263
[7] Chan V.S. *et al* 2010 *Fusion Sci. Technol.* **57** 66
[8] Magnani E. *et al* 2009 *Fus. Eng. Des.* **84** 1238
[9] Hiwatari R., Okano K., Asaoka Y., Shinya K. and Ogawa Y. 2005 *Nucl. Fusion* **45** 96
[10] Dean S.O., Baker C.C., Cohn D.R. and Kinkead S.D. 1991 *J. Fusion Energy* **10** 197–206
[11] Goldston R.J. 2010 A pilot plant: the fastest path to commercial fusion energy *Technical Report* PPPL-4501
[12] ARIES Program Public Information Site (http://www-ferp.ucsd.edu/ARIES/DOCS/final-report.shtml)
[13] Abdou M.A. *et al* 1996 *Fusion Technol.* **29** 1
[14] El-Guebaly L.A. and The ARIES Team 2003 *Fusion Eng. Des.* **65** 263
[15] Doyle E. *et al* 2007 *Nucl. Fusion* **47** S18
[16] Greenwald M. 2002 *Plasma Phys. Control. Fusion* **44** R27
[17] Yamada H. *et al* 2004 *Nucl. Fusion* **45** 1684
[18] Duchateau J. 2006 *Fusion Eng. Des.* **81** 2351
[19] Salpietro E. 2006 *Supercond. Sci. Technol.* **19** S84
[20] Schultz J.H., Radovinsky A. and Titus P. 2004 Description of the TF magnet and FIRE-SCSS (FIRE-6) design concept *PSFC Report* PSFC/RR-04-3
[21] Bromberg L. 2010 personal communication
[22] Raffray A.R. *et al* 2007 *Fusion Eng. Des.* **82** 2696
[23] Sabbagh S.A. *et al* 2010 *Proc. 23rd Int. Conf. on Fusion Energy 2010 (Daejeon, South Korea 2010)* (Vienna: IAEA) CD-ROM file [EX-S/5-5] and http://www-pub.iaea.org/MTCD/Meetings/cn180_papers.asp
[24] Giancarli L., Ferrari M., Futterer M.A. and Malang S. 2000 *Fusion Eng. Des.* **49–50** 445
[25] Boccaccini L.V. *et al* 2004 *J. Nucl. Mater.* **329-333** 148
[26] Garcia J. *et al* 2008 *Plasma Phys. Control. Fusion* **50** 124032
[27] Kessel C.E. *et al* 2007 *Nucl. Fusion* **47** 1274
[28] Murakami M. *et al* 2010 *Proc. 23rd Int. Conf. on Fusion Energy 2010 (Daejeon, South Korea 2010)* (Vienna: IAEA) CD-ROM file [ITR/P1-35] and http://www-pub.iaea.org/MTCD/Meetings/cn180_papers.asp
[29] Loarte A. *et al* 2007 *Nucl. Fusion* **47** S203
[30] Reiersen W. *et al* 2003 *Fusion Eng. Des.* **65** 303
[31] Neilson G.H. *et al Proc. 23rd Int. Conf. on Fusion Energy 2010 (Daejeon, South Korea 2010)* (Vienna: IAEA) CD-ROM file [FTP/P6-06] and http://www-pub.iaea.org/MTCD/Meetings/cn180_papers.asp
[32] Maisonnier D. 2008 *Fusion Eng. Des.* **83** 858
[33] Menard J.E. *et al* 2004 *Phys. Plasmas* **11** 639
[34] Holcomb C.T. *et al* 2009 *Phys. Plasmas* **16** 056116
[35] Menard J.E. *et al* 2006 *Phys. Rev. Lett.* **97** 095002
[36] Gates D.A. *et al* 2006 *Phys. Plasmas* **13** 056122
[37] Maingi R. *et al* 2010 *Phys. Rev. Lett.* **25** 135004
[38] Menard J.E. *et al* 2010 Physics design of the NSTX upgrade, Paper P2.106 *Proc. 37th EPS Conf. Plasma Physics (Dublin, Ireland 2010)* http://ocs.ciemat.es/EPS2010PAP/pdf/P2.106.pdf
[39] Watanabe K.Y. *et al* 2005 *Nucl. Fusion* **45** 1247
[40] Mccormick K. *et al* 2002 *Phys. Rev. Lett.* **89** 015001
[41] Start D.F.H., Cordey J.G. and Jones E.M. 1980 *Plasma Phys.* **22** 303
[42] Oikawa T. *et al* 2001 *Nucl. Fusion* **41** 1575
[43] Hemsworth R.S. 2003 *Nucl. Fusion* **43** 851
[44] Kulygin V.M. *et al* 2001 *Nucl. Fusion* **41** 355
[45] Kovari M. and Crowley B. 2010 *Fusion Eng. Des.* **85** 745
[46] Ridolfini V.P. *et al* 2005 *Nucl. Fusion* **45** 1085
[47] Imai T. *et al* 1990 *Fusion Eng. Des.* **13** 177
[48] Ekedahl A. *et al* 2009 *Plasma Phys. Control. Fusion* **51** 044001
[49] Norajitra P. *et al* 2007 *J. Nucl. Mater.* **367–370** 1416
[50] Labombard B. *et al* 2011 *Phys. Plasmas* **18** 056104
[51] Lasnier C.J. *et al* 2011 *J. Nucl. Mater.* at press (doi:10.1016/j.jnucmat.2011.01.029)
[52] Gray T.K. *et al* 2011 *J. Nucl. Mater.* an press (doi:10.1016/j.jnucmat.2010.12.008)
[53] Goldston R.J. 2011 Heuristic drift-based model of the power scrape-off width in H-mode tokamaks *Technical Report* PPPL-4619, 2011 *Nucl. Fusion* submitted
[54] Kotschenreuther M., Valanju P.M., Mahajan S.M. and Wiley J.C. 2007 *Phys. Plasmas* **14** 072502
[55] Umansky M.V., Bulmer R.H., Cohen R.H., Rognlien T.D. and Ryutov D.D. 2009 *Nucl. Fusion* **49** 075005
[56] Valanju P.M., Kotschenreuther M., Mahajan S.M. and Canik J. 2009 *Phys. Plasmas* **16** 056110
[57] Ryutov D.D. 2007 *Phys. Plasmas* **14** 064502
[58] Soukhanovskii V.A. *et al* 2009 *Nucl. Fusion* **49** 095025
[59] Soukhanovskii V.A. *et al* 2011 *Nucl. Fusion* **51** 012001
[60] Rosenbluth M.N. and Putvinski S.V. 1997 *Nucl. Fusion* **37** 1356
[61] Wesley J.C. *et al* 2006 *Proc. 21st Int. Conf. on Fusion Energy 2006 (Chengdu, China 2006)* (Vienna: IAEA) CD-ROM file [IT/P1-21] and http://www-naweb.iaea.org/napc/physics/FEC/FEC2006/html/index.htm